Chemical Engineering Journal 222 (2013) 240–247

Contents lists available at SciVerse ScienceDirect

Chemical Engineering Journal

journal homepage: www.elsevier.com/locate/cej

High efficient removal of Cu(II) by a chelating resin from strong acidic solutions: Complex formation and DFT certification

Jie Gao [a], Fuqiang Liu [a,b,*], Panpan Ling [c], Jintao Lei [a], Lanjuan Li [a], Chenghui Li [b], Aimin Li [a]

[a] State Key Laboratory of Pollution Control and Resources Reuse, School of the Environment, Nanjing University, Nanjing 210046, PR China
[b] Coordination Chemistry Institute of Nanjing University, Nanjing 210093, PR China
[c] Lianyungang Institute of Environmental Science, Lianyungang 222001, PR China

HIGHLIGHTS

- Efficient removal of Cu(II) by a novel resin from strong acid solutions was explored.
- Interaction mechanisms under different acidity were depicted with the help of XPS.
- Preponderant geometric structure of complex in strong acid media was affirmed by DFT.
- Three-dimensional conformation of complex at active sites in nanopores was simulated.
- Method without neutralization to recover metal ions from strong acids was speculated.

ARTICLE INFO

Article history:
Received 5 December 2012
Received in revised form 15 February 2013
Accepted 16 February 2013
Available online 22 February 2013

Keywords:
Chelating resin
Cu(II)
Complex formation
Interaction mechanisms
Density-Functional-Theory

ABSTRACT

The novel chelating resin Dowex M-4195 was selected and applied to investigate the static adsorption properties and interaction nature toward aqueous Cu(II) from acid solutions. The isotherm data could be well described by Langmuir model, and the kinetic curves could be successfully fitted with the pseudo-second-order equation. In strong acid solutions at the pH-value of 2, the obtained adsorption capacity was 1.592 mmol/g, about 50% more than that at the higher pH-value of 5. The adsorption mechanism of Cu(II) onto Dowex M-4195, especially at the pH-value of 2, were further explored using the Density-Functional-Theory. The theoretical calculations confirmed the three nitrogen atoms would be all involved in the coordination with tridentate complex and thus the two five-member ring structure could be achieved. Additionally, the XPS spectra testified the involvement of nitrogen atoms, which told the coordination ratio might be 1:1. Whereas, in weak acidic solutions at the pH value of 5, the ion exchange mechanism involving the protonated pyridine of solid matrix and Cu(II) was dominant. Consequently, high efficient removal of Cu(II) especially from strong acidic solutions could be achieved, an indication of a potential and preponderant new method to recover heavy metals from acidic effluents without sufficient neutralization pretreatment.

1. Introduction

Heavy metals from industrial wastewater have been excessively released into the aquatic ecosystems and thus created more and more comprehensive concern around the world. Unlike organic pollutants, heavy metals can be accumulated in the environment and living organisms for a prolonged time, and cause various disorders and diseases ultimately [1–3]. Copper together with other heavy metals, is considered as high relative mammalian toxic which could often be detected in chemical effluents. However, with the rapid industrialization, too many Cu-based chemicals from copper mining activities, smelting, electroplating industries, and brass manufacture make copper-pollution more severe [2,4,5]. As is known to all, the continued inhalation of copper containing sprays is relevance with an increase in lung cancer among exposed workers, therefore the removal of copper can be paid significant attention [6]. As a matter of fact, such methods to remove Cu(II) from industrial wastewaters, as chemical precipitation, coagulation [7], ion exchange [8], electrolytic methods [9], reverse osmosis [10] and adsorption [11] were reported earlier. Among them, adsorption is considered more effective especially in the trace amounts cases for its far higher capacity and selectivity [3,12]. So far, a large amount of materials have been used as adsorbents, such as activated carbon [13,14], activated alumina [15], red mud [16],

* Corresponding author at: State Key Laboratory of Pollution Control and Resources Reuse, School of the Environment, Nanjing University, Nanjing 210046, PR China. Tel./fax: +86 25 89680377.
E-mail address: jogia@163.com (F.Q. Liu).

1385-8947/$ - see front matter © 2013 Elsevier B.V. All rights reserved.
http://dx.doi.org/10.1016/j.cej.2013.02.055

layered double hydroxides [17], fibrous adsorbents [18] and resins [1,4]. However, most adsorbents could only be used in media of mild pH values [19–21] which requires complex neutralization pretreatment for the strong acidic Cu-based industrial wastewater. For instance, iminodiacetic acid chelating resin (IDA) and dithiocarbamate chelating resin (DTC) have been used to remove Cu(II) from aquatic media [22–24] due to their large adsorption capacity, high selectivity, excellent mechanical character and easy regeneration [25–28]. Nevertheless, the DTC chelating resins are solely used in weak acidic environment [29,30], while the IDA resins could only be applied under alkaline condition due to their weak acid characters [31]. Necessarily, the selective removal of metal ions from strong acid media is recognized as a difficult task for almost all the above-mentioned Cu-based industries.

Thus, more effective chelating resins especially under lower pH-values should be discovered and detected in details. Diniz [32] and Nagib [33] have reported the novel chelating resin Dowex M-4195 which owned an unusual ability in the removal of Cu(II) even under lower pH values. As reported earlier, the structure of Dowex M-4195 is based on bispicolylamine, which is attached to a polystyrene divinylbenzene matrix. Bispicolylamine or bis(2-pyridylmethyl) amine is a heterocyclic polyamine with three nitrogen donor atoms, as shown in Scheme 1.

However, relatively less work has been paid on the nature of these nitrogen-containing chelating resins before and after their interaction with heavy metals, which are of great significance for the design of highly effective chelating resin [26,34,35]. As an important supplement to the experimental investigation, the theoretical calculation as well as refined analysis, could overcome the problems connected with the experimental techniques and provide excellent complement [36]. It could offer necessary information on the coordination modes, structures, as well as the binding abilities of the chelating resin towards heavy metal ions [37]. Furthermore, the development of Density-Functional-Theory (DFT) provides a new credible tool in this field [38–40]. Particularly, DFT method has been proven to be computationally efficient and satisfactory for the prediction of molecular properties after the interactions especially involving transitional metal systems [41–43].

In this work, the novel chelating resin Dowex M-4195 was selected as the exclusive adsorbent. The static adsorption performance including equilibria and kinetics toward Cu(II) were herein explored and described by different models. The fact was that the far higher adsorption capacity in strong acid solutions than that in weak acid solutions for Cu(II) onto Dowex M-4195, which maybe lead to a potential and preponderant new method to recover heavy metals from common strong acidic industrial wastewater without sufficient neutralization pretreatment. The aim of this work was to investigate the interactive mechanisms under different pH values with the help of XPS and DFT. The complex formed in strong acid solutions and the three-dimensional interactive conformation was significant to explore the micromechanisms for various heterogeneous materials.

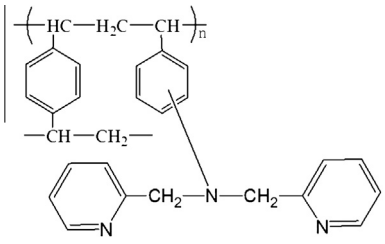

Scheme 1. Structure of Dowex M-4195.

2. Methods

2.1. Materials

Sodium hydroxide, nitric acid, and copper nitrate were all analytical reagents and purchased from Nanjing NingShi Reagent Company (Nanjing, JiangSu, PRC).

Dowex M-4195 was manufactured by Dow Chemical (Midland, MI, USA), and purchased from Supelco–Sigma Aldrich Division (Bellefonte, PA, USA).

2.2. Characterization of Dowex M-4195

Element analysis (EA, Elemental Vario MICRO) of Dowex M-4195 was carried out in order to determine the amount of ligands available in the matrix, and the functional groups were obtained by Fourier transform infrared spectroscopy (FT-IR, Nicolet 170 SX). The specific surface area and mean pore size distribution (PSD, ASAP 2020 M+C) were measured using the nitrogen gas adsorption/desorption method. The surface chemical state of the resin and surface elemental composition before and after the interaction with Cu(II) were further analyzed by electron spectroscopy analysis (XPS, ESCALAB 250).

2.3. Static tests

2.3.1. Isotherms

Equilibrium adsorption of Cu(II) was performed at three different temperatures (283 K, 303 K, and 323 K) in batch systems. Adsorption isotherms were performed with different initial concentrations in the range of 0.5–5.0 mmol/L of Cu(II) while keeping the dry resin amount at the certain value of 1.0 g/L. The residual concentrations of Cu(II) in solutions were determined using a flame atomic absorption spectrophotometer (AAS, TAS-990, Beijing Pgeneral Co.). The initial pH values of the sample solutions were adjusted at 5 and 2 by HNO_3 or NaOH. All pH values were measured with a PHS-3C digital pH meter. The amount of metal ion adsorbed per unit mass of the resin could be determined with the following expression as:

$$Q_e = \frac{(C_0 - C_e) \times V}{W} \tag{1}$$

where C_0 and C_e are the concentrations of the metal ion in the aqueous phase before and after the equilibration, respectively (mmol/L). V is the volume of the aqueous phase (L), W is the amount of the resin used (g) and Q_e is the equilibration adsorption capacity (mmol/g).

The Langmuir and Freundlich isotherm models are employed as the form of:

$$\frac{C_e}{Q_e} = \frac{C_e}{Q_0} + \frac{1}{Q_0 b} \tag{2}$$

where C_e is the equilibrium concentration (mmol/L), Q_e is the amount of adsorbed material at equilibrium (mmol/g), b is the affinity parameter or Langmuir adsorption constant (L/mmol) which reflects the free energy of adsorption, and Q_0 is the capacity parameter (mmol/g) [44,45].

$$Q_e = K_f C_e^{1/n} \tag{3}$$

where Q_e is the equilibrium capacity (mmol/g), C_e is the equilibrium concentration (mmol/L), K_f and n are the constant isotherm parameters.

2.3.2. Kinetics

The rate of loading of metal ion on the resins could be determined by kinetic tests. Certain amount (1000 mL) of metal ion solution with the initial concentration of 1 mmol/L was introduced with 1.000 g resin at 303 K. The mixture solution was adjusted to the initial pH value of 5 and 2, and then mechanically stirred under 120 rpm. The samples (1 mL) were withdrawn at predetermined intervals for the analysis with AAS.

The kinetic parameters of metal ion adsorption are important for designing adsorption systems, and pseudo-first-order and pseudo-second-order kinetic models can usually be applied to describe the kinetic adsorption process.

The pseudo-first-order and pseudo-second-order kinetic models are given as the form of:

$$\log(Q_e - Q_t) = \log Q_e - \frac{k_1 t}{2.303} \quad (4)$$

$$\frac{t}{Q_t} = \frac{1}{(k_2 Q_e^2)} + \frac{t}{Q_e} \quad (5)$$

$$h = k_2 Q_e^2 \quad (6)$$

where Q_t is the adsorption capacity at time t (mmol/g), Q_e is the adsorption capacity at equilibrium (mmol/g), h is the initial adsorption rate constant of pseudo-second-order (mmol/g/min), and k_1, k_2 are the adsorption rate constants of pseudo-first-order (min^{-1}), pseudo-second-order (g/mmol/min), respectively [46].

2.4. Computational details

All the calculations were based on DFT and carried out using the Gaussian 03 suit of programs. Geometries of the chelating resin model and its metal complexes were fully optimized using DFT method with the B3LYP hybrid density functional theory. The C, H and N atoms used 6-31+G(d) basis set, while the metal ions were depicted by LANL2DZ relativistic pseudo potentials, which were proved most credible for the transition-metal ligands [41–43]. All possible geometries were fully optimized without the imposition of symmetry constraints. Harmonic vibrational frequencies were calculated at the same level to ensure that the stationary points be true minima.

Binding energies (ΔE), as the energy differences between the total energy of the complex and those of the individual molecules, were calculated by Eq. (7). Polarizable continuum model (PCM) was applied to evaluate the solvent effect of water on the binding energies [36].

$$\Delta E = E(\text{complex}) - [E(\text{chelating resin}) + E(\text{metal})] \quad (7)$$

where E is the total energy obtained by the single point energy calculations at the B3LYP/6-31+G(d,p)//B3LYP/6-31+G(d) (LANL2DZ for metal ions) level.

3. Results and discussion

3.1. Characterization of Dowex M-4195

3.1.1. EA results

EA results including C, H, and N of Dowex M-4195 were tabulated in Table 1. The content of nitrogen in the resin was 9.4%, corresponding to the functional group capacity of 2.24 mmol/g.

Table 1
EA of the resin Dowex M-4195.

Resin	Element content (%)		
	C	H	N
Dowex M-4195	80.63	7.42	9.40

3.1.2. FT-IR spectra

The FT-IR spectra of Dowex M-4195 were presented in Fig. 1. The adsorption bands near 1363 cm^{-1} and 1433 cm^{-1} corresponded to the stretching vibrations of C—N, and the adsorption feature near 1590 cm^{-1} was caused by C=N of pyridine. Adsorption peak of C—H occurred between 2920 cm^{-1} and 760 cm^{-1} [47–49]. Thus, the functional groups of Dowex M-4195 were confirmed to be pyridine and aliphatic amine.

3.1.3. PSD analysis

The adsorption and desorption isotherms of nitrogen at 77 K on Dowex M-4195 during PSD analysis were shown in Fig. 2. The isotherms displayed a Type IV profile according to the IUPAC classification with hysteretic loops in relative pressure higher than 0.9 [50], indicating that the pores were mostly mesoporous and macroporous. Distribution curve demonstrated that the porous distribution was relatively concentrated and the porous size of resin was mainly mesopores of about 40 nm. Such porous characteristics might contribute to the diffusion of those metal ions with only several nm magnitudes in the adsorption process.

3.2. Static investigation

3.2.1. Equilibrium isotherms

The adsorption isotherms for Dowex M-4195 could be well described by both Langmuir and Freundlich models. The amount of Cu(II) adsorbed per unit mass of Dowex M-4195 increased with the initial metal concentration and temperature as expected. Whereas, the Langmuir model could describe all isotherm data with more success, as could be found in Table 2. Equilibrium adsorption capacity increased from 0.796 mmol/g to 1.592 mmol/g along with the decrease in pH-value from 5 to 2 at 303 K. Similarly, the Langmuir adsorption constant b increased with the decline in pH-value, illustrating that Dowex M-4195 owned greater affinity with Cu(II) even at lower pH values. The favorable properties in acid solution might be associated with the unique chemical characters of Dowex M-4195.

3.2.2. Adsorption kinetics

The pseudo-first-order and pseudo-second-order models were used to interpret the adsorption kinetics, and the fitting curves and key parameters could be found in Fig. 3 and Table 3, respectively. The pseudo-second-order kinetic model could succeed in describing the kinetic curves, which demonstrated that the adsorption rate of metal ions extremely depended on the concentration of

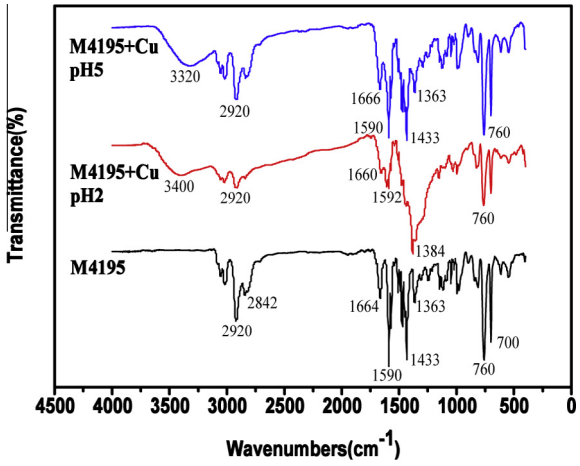

Fig. 1. FT-IR spectra of Dowex M-4195 before and after loaded with Cu(II).

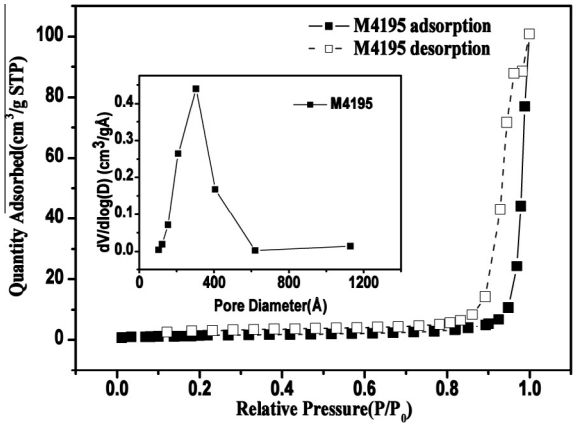

Fig. 2. N_2 adsorption/desorption isotherms and PSD curves of Dowex M-4195.

Table 2
Constant parameters of the Langmuir and Freundlich isotherms.

Resin	pH-value	T (K)	Langmuir constants			Freundlich constants		
			Q_0	b	r^2	K_f	n	r^2
Dowex M-4195	5	283	0.799	0.244	0.996	0.161	1.529	0.990
		303	0.796	0.304	0.996	0.194	1.675	0.990
		323	1.341	0.226	0.999	0.245	1.439	0.994
	2	283	1.394	0.376	0.998	0.370	1.603	0.991
		303	1.592	0.414	0.998	0.524	1.934	0.994
		323	2.140	0.387	0.997	0.696	1.938	0.996

ions at the adsorbent surface, as reported in an earlier literature [46].

As could be seen from Fig. 3 and Table 3, the adsorption equilibrium could be obtained after 5 h at the initial pH-value of 5, versus 24 h at 2. So, the lower initial pH-value of the solution was, the longer the adsorption equilibrium time could be achieved. Further, such deep decline as 57.4% and 98.3% in the initial adsorption rate (the value of h) and the total adsorption rate constant (the value of k_2) could be found with the initial pH-value decreasing from 5 to 2.

Diniz [32] discovered that all of the three nitrogen atoms on the functional group of Dowex M-4195 would be protonated at the lower pH values, and only one of the pyridyl nitrogens was protonated in the middle pH values. Under the pH-value of 5, the adsorption of Cu(II) on Dowex M-4195 was dominated by ion exchange with protonated pyridyl nitrogens, so the adsorption rate

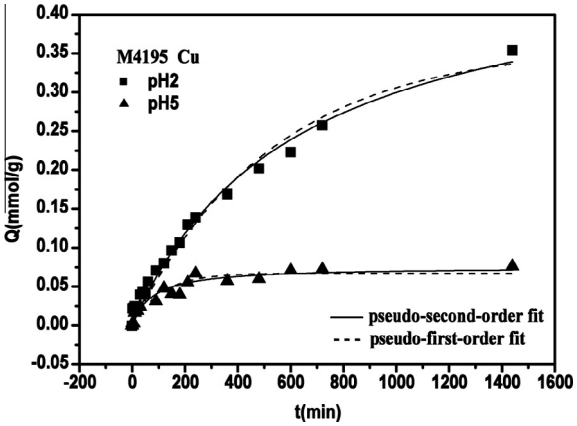

Fig. 3. Effect of the adsorption time on the capacities for Cu(II) adsorption by Dowex M-4195.

Table 3
Adsorption kinetic parameters of Dowex M-4195.

Resin	pH-Value	Pseudo-first-order			Pseudo-second-order			
		Q_e	k_1	r^2	Q_e	k_2	h	r^2
Dowex M-4195	5	0.067	0.009	0.890	0.075	0.172	0.001	0.926
	2	0.360	0.002	0.977	0.485	0.003	7×10^{-4}	0.985

was more rapid. In addition, for more protons coexisted under the pH-value of 2, ion exchange process was synchronously weakened. Consequently, the adsorption process for Cu(II) was dominated by chelation, with the far slower adsorption rate.

3.3. Interaction mechanism

3.3.1. Interpretation of FT-IR analysis

The distinct interaction effects after Cu(II) loaded on the solid phase at different pH values were simultaneously displayed in Fig. 1. The broad adsorption band near 3400 cm^{-1} appeared, which was probably due to the superposition of the adsorption of the stretching vibrations of the functional groups [51]. The appearance of the new peak at 1384 cm^{-1} corresponded to the stretching vibration of NO_2 in the NO_3^- ions [20]. Due to the adsorption of Cu(II) on the resin by interacting with the nitrogen ligands, the NO_3^- groups would incorporate with the Cu(II)–resin complex to neutralize the positive charges introduced by the copper ion. Hence, it was conceivable that NO_3^- ions were synchronously adsorbed onto Dowex M-4195 to neutralize the electrical charges of the solid beads. The changes caused by the load of Cu(II) at the pH-value of 2 should be attributed to the coordination process involving the pyridine groups and aliphatic amine groups. As for pH-value of 5, such changes could not be observed obviously, implying that ion exchange rather than coordination should be predominant.

3.3.2. Interpretation of XPS analysis

The XPS spectra of Dowex M-4195 before and after loaded with Cu(II) under different pH–values were displayed in Fig. 4. The N1s core-level XPS spectra of the M4195 could be fitted by two peaks at 399.39 eV and 400.6 eV, which corresponded to the nitrogens in the C═N group and C—N group, respectively [52,53]. Notably, the new peaks at the BE of 400.09 eV and 399.19 eV, were not created for pH 2 but for pH 5, and the shift for the latter could be negligible with less than 0.05 eV, hence it could be indicated the nitrogens in aliphatic and pyridine amine were not involved in the interaction processes. Whereas, the obvious shift for pyridine nitrogen and aliphatic nitrogen at the pH-value of 2 were 0.18 eV and 0.63 eV. So, at the lower pH-value of 2, the lone pair of electrons in the nitrogen atom of the amine group could be donated to form a shared bond between the atoms of Cu and N.

3.3.3. Theoretical investigation for metal complexes

3.3.3.1. Interaction modes. Under the temperature of 323 K and the pH-value of 2, the adsorption capacity of Dowex M-4195 towards Cu(II) was 2.140 mmol/g. Based on the content of nitrogen element of 6.71 mmol/g, the mole ratio for N versus Cu(II) was 3: 1. As known to all, such heavy metals as Cu(II) owned a maximum coordinated number of six and may adopt octahedral complexing arrangement. Since Cu(II) with nine *d*-electrons ($t2$ g and $e2$ g) constituted a classical regular octahedral geometry, the favorable active sites for coordination should be the electron rich nitrogen atoms [49]. As agreed with the FT-IR and XPS spectra, the nitrogen atoms were concluded to be participated in the complexing process. However, it could not be confirmed whether all the pyridine nitrogen atoms were participated in the chelation interaction.

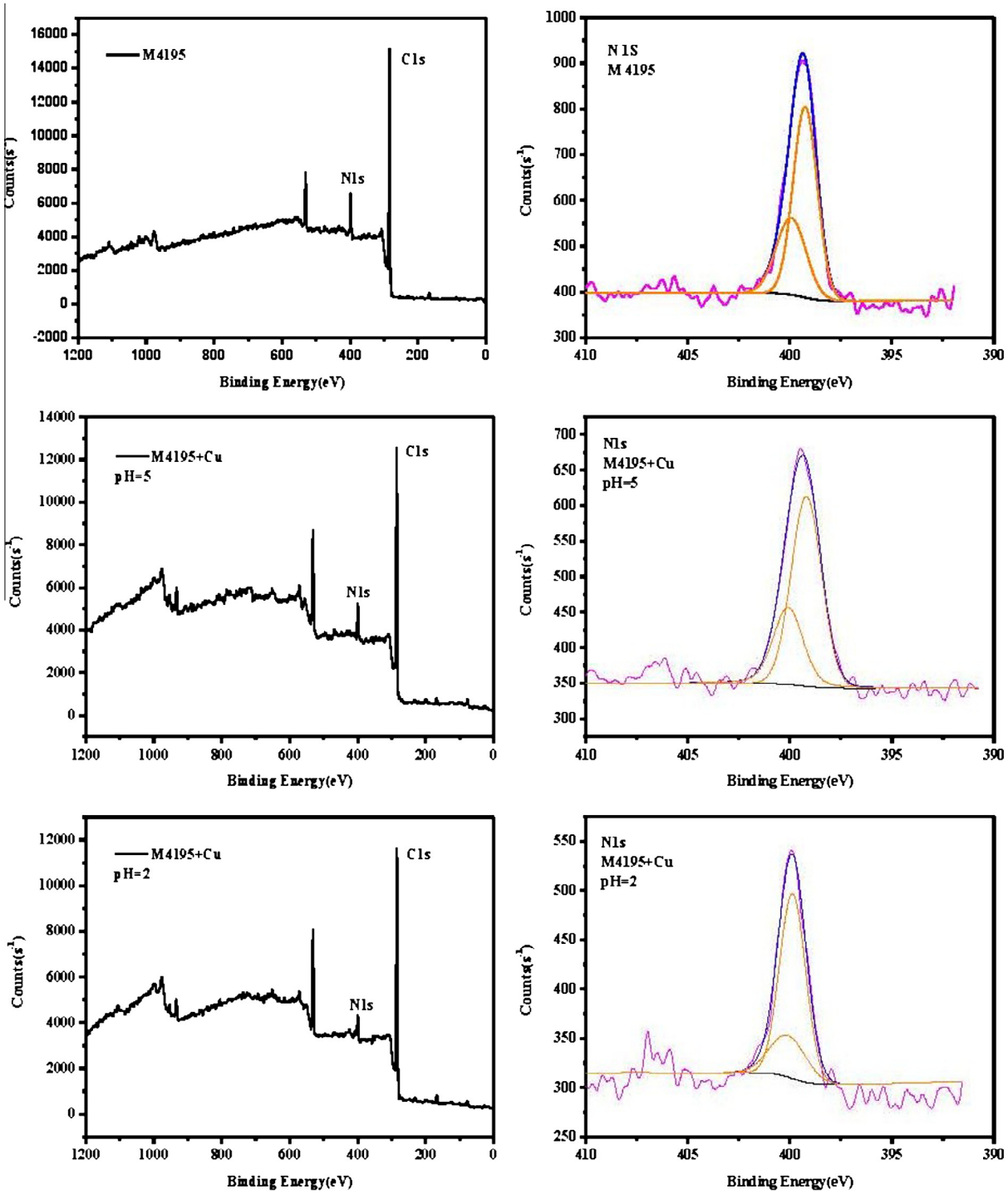

Fig. 4. XPS analysis of Dowex M-4195 before and after loaded with Cu(II).

Considering the cases of one or two pyridine nitrogen atoms involved, two possible configurations were presented in Scheme 2.

Under the temperature of 303 K and the pH-value of 5, the adsorption capacity of Dowex M-4195 towards Cu(II) was 0.796 mmol/g, half of that under the pH-value of 2. Thus, all of the six nitrogen atoms were related to the interaction with only one Cu ion in the former case. Compared to the condition of pH 2, the surface of the resin was partially protonated [54] and ion exchange was more likely to occur due to the less hydrogen inhibitory [55] at the pH-value of 5. Additionally, there was no evidence for chelation in FT-IR and XPS spectra. Consequently, ion exchange took place between protonated hydrogen ions and Cu ions [56]. It could be concluded that ion exchange mechanism was dominant in the case of pH-value of 5, as was shown in Scheme 3.

3.3.3.2. Chelation mechanisms. The geometric structure of the functional group for Dowex M-4195 was optimized at B3LYP/6-31+G(d) level of theory as shown in Fig. 5. Furthermore, the optimized structures of possible resin–metal complexes were depicted in Fig. 6. And the main structural parameters were tabulated in Table 4.

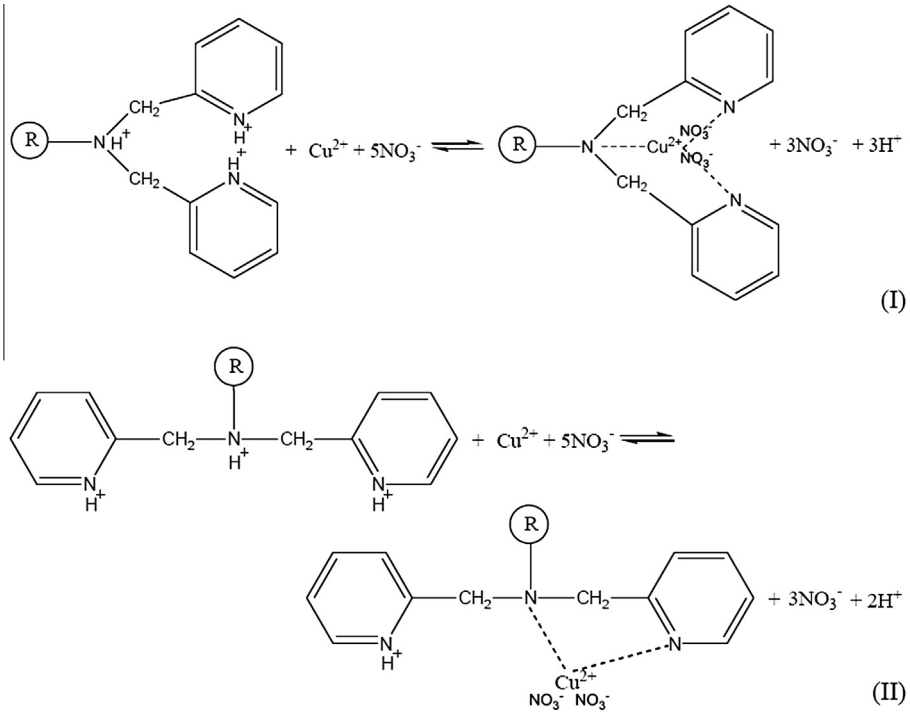

Scheme 2. The interaction modes of Dowex M-4195 towards Cu(II) (pH = 2).

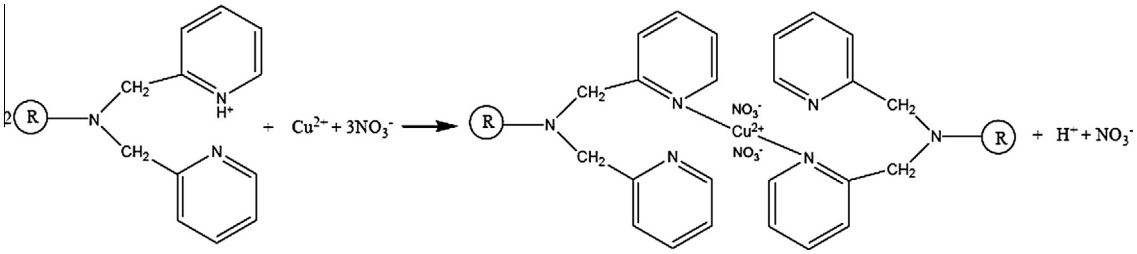

Scheme 3. The interaction of Dowex M-4195 towards Cu(II) (pH = 5).

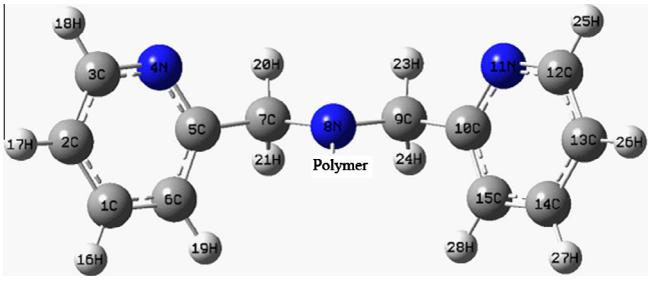

Fig. 5. The optimized structure of Dowex M-4195.

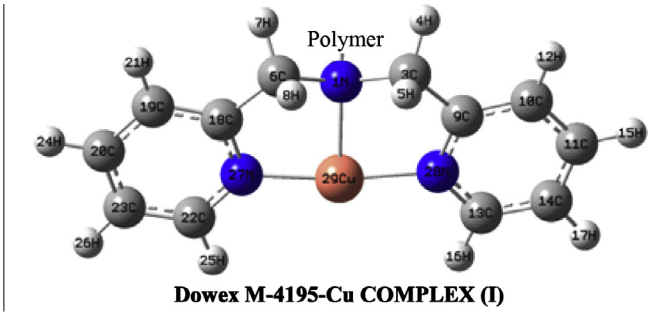

Fig. 6. The complex structures of Cu(II) coordinated with Dowex M-4195 after optimization.

Geometrical changes of complexes were mainly due to the presence of metal ions, and differed according to their configuration [57]. The coordinated atoms could exert remarkable influences upon metal-chelator bonding and liability of other bonds within a complex [49]. As could be found in Fig. 6, for COMPLEX (I), it was tridentate and more stable because of the two five-member ring structure. Whereas for COMPLEX (II), the five-member ring structure was brokened, which was an indicative of a less stable structure in a certain extent.

Comparing the two complexes with the primary chemical groups, significant changes occurred not only in the bond lengths,

Table 4
Selected optimized geometrical parameters of resin and complexes.

	M-4195		Complex (I)		Complex (II)	
Bond length (Å)	N8—C7	1.470	N1—C6	1.491	N13—C10	1.502
	N8—C9	1.470	N1—C6	1.491	N13—C15	1.490
			Cu29—N1	2.037	Cu29—N27	1.968
			Cu29—N27	1.930	Cu29—N13	2.068
			Cu29—N28	1.929		
Bond angle (°)	C7—N8—C9	114.86	C6—N1—C3	119.50	C10—N13—C15	115.68
	C5—C7—N8	111.19	C18—C6—N1	109.83	C2—C10—N13	112.16
			N1—Cu29—N27	85.93		
			N1—Cu29—N28	85.92		
			Cu29—N27—C18	112.93	Cu29—N27—C2	110.38
Dihedral angle(°)	N4—C5—C7—N8	102.92	N27—C18—C6—N1	27.04	N27—C2—C10—N13	−30.68
	N8—C9—C10—N11	−102.97	N1—C3—C9—N28	−27.18	N13—C5—C18—N28	63.54
			N27—Cu29—N1—N28	176.80		

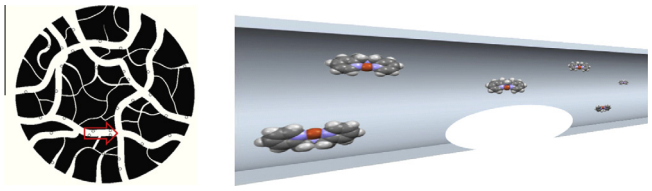

Fig. 7. Simulated sketch of COMPLEX (I) on solid matrix.

but also in the bond angles and dihedral angles, which displayed the magnitude of asymmetric distortion. As could be seen from Table 4, the interaction with metal ions led to the longer distance between aliphatic amine and adjacent carbon atoms and the larger bond angle in the optimized steady state.

As for the differences in COMPLEX (I) and COMPLEX (II), the bond length in the range of 1.929–2.037 Å for the former was a little shorter than 1.968–2.068 Å for the latter. Meanwhile, the change in the bond angles of 4.64° for the former was far larger, versus only 0.82° for the latter. Further, the binding energy for COMPLEX (I) was −1982.2 KJ/mol, versus −1795.8 KJ/mol for COMPLEX (II), so the former was the minimum energy complex configuration. To add further relevance to the adsorption processes, the solvent effect of water was estimated by the polarizable continuum model. Results indicated that the existence of water produced insignificant effect on the equilibrium geometries of the complexes. The binding energy for COMPLEX (I) was −2588.7 KJ/mol, versus −2428.5 KJ/mol for COMPLEX (II), so the former was still the minimum energy complex configuration. Obviously, the presence of solvent did not change the order of binding energies. Hence, COMPLEX (I) was confirmed more stable for its shorter bond lengths, larger bond angle changes and lower binding energy. Considering the shorter distance between metal ion and pyridine nitrogen than aliphatic nitrogen, pyridine nitrogens could assuredly play significant roles in the processes tested. As a matter of fact, pyridine N atoms were proved the electron donors with stronger chelating ability by titrations in earlier literatures [58,59].

Combining the XPS application and DFT calculation, the dominant and stable chelating interaction under pH-value of 2 involved three nitrogen atoms of Dowex M-4195 and Cu(II) [60–62]. Emphatically, the three-dimensional interaction at the active sites in solid nanopores involving the coordinated pontes for COMPLEX (I) were simulated in Fig. 7, which legibly revealed the tridentate complex with two five-member ring structure.

4. Conclusion

Dowex M-4195 is a special resin which could be applied to recover heavy metals from strong acidic media which maybe lead to a potential and preponderant new method to recover heavy metals from common strong acidic industrial wastewater without sufficient neutralization pretreatment. The resin shows greater adsorption capacity and slower adsorption constant toward Cu(II) at pH of 2 than that at pH of 5 which accords with different interaction mechanisms. As for pH of 2, the physical and chemical characterization together with DFT prove that Cu(II) and nitrogen atoms in pyridine and aliphatic amine coordinate with a ratio of 1:1, but for pH of 5, the main process is ion-exchange between the Cu(II) in solution and the protonated pyridine of the chelating resin Dowex M-4195.

Acknowledgements

The authors gratefully acknowledge generous support provided by the State Key Program of National Natural Science (Grant No. 50938004), the Resources Key Subject of National High Technology Research & Development Project (863 Project, Grant No. 2009AA06Z315 and SQ2009AA06XK1482331), PR China, the National Natural Science Foundation of PR China (No. 51078178) and the Discipline Crossing Foundation of Nanjing University.

References

[1] H.A. Saadeh, E.A. Abu Shairah, N. Charef, M.S. Mubarak, Synthesis and adsorption properties, toward some heavy metal ions, of a new polystyrene-based terpyridine polymer, J. Appl. Polym. Sci. 124 (2012) 2717–2724.
[2] F.M. Pellera, A. Giannis, D. Kalderis, K. Anastasiadou, R. Stegmann, J.Y. Wang, E. Gidarakos, Adsorption of Cu(II) ions from aqueous solutions on biochars prepared from agricultural by-products, J. Environ. Manage. 96 (2012) 35–42.
[3] M. Rajiv Gandhi, S. Meenakshi, Preparation and characterization of silica gel/chitosan composite for the removal of Cu(II) and Pb(II), Int. J. Biol. Macromol. 50 (2012) 650–657.
[4] R. Kumar, S.K. Jain, R.K. Misra, M. Kachchwaha, P.K. Khatri, Aqueous heavy metals removal by adsorption on beta-diketone-functionalized styrene–divinylbenzene copolymeric resin, Int. J. Environ. Sci. Technol. 9 (2012) 79–84.
[5] I.Y. Goon, C. Zhang, M. Lim, J.J. Gooding, R. Amal, Controlled fabrication of polyethylenimine-functionalized magnetic nanoparticles for the sequestration and quantification of free Cu(2+), Langmuir 26 (2010) 12247–12252.
[6] J. Duan, Q. Lu, R. Chen, Y. Duan, L. Wang, L. Gao, S. Pan, Synthesis of a novel flocculant on the basis of crosslinked Konjac glucomannan-graft-polyacrylamide-co-sodium xanthate and its application in removal of Cu^{2+} ion, Carbohydr. Polym. 80 (2010) 436–441.
[7] F. Fu, Q. Wang, Removal of heavy metal ions from wastewaters: a review, J. Environ. Manage. 92 (2011) 407–418.
[8] M.A. Barakat, New trends in removing heavy metals from industrial wastewater, Arab. J. Chem. 4 (2011) 361–377.
[9] N. Meunier, P. Drogui, C. Montané, R. Hausler, G. Mercier, J.F. Blais, Comparison between electrocoagulation and chemical precipitation for metals removal from acidic soil leachate, J. Hazard. Mater. 137 (2006) 581–590.
[10] F. Liu, G. Zhang, Q. Meng, H. Zhang, Performance of nanofiltration and reverse osmosis membranes in metal effluent treatment, Chin. J. Chem. Eng 16 (2008) 441–445.
[11] C.-S. Zhu, L.-P. Wang, W.-b. Chen, Removal of Cu(II) from aqueous solution by agricultural by-product: peanut hull, J. Hazard. Mater. 168 (2009) 739–746.

[12] C.G. Rocha, D.A.M. Zaia, R.V.d.S. Alfaya, A.A.d.S. Alfaya, Use of rice straw as biosorbent for removal of Cu(II), Zn(II), Cd(II) and Hg(II) ions in industrial effluents, J. Hazard. Mater. 166 (2009) 383–388.
[13] M.A.A. Zaini, Y. Amano, M. Machida, Adsorption of heavy metals onto activated carbons derived from polyacrylonitrile fiber, J. Hazard. Mater. 180 (2010) 552–560.
[14] M.C. Basso, A.L. Cukierman, Wastewater treatment by chemically activated carbons from giant reed: effect of the activation atmosphere on properties and adsorptive behavior, Sep. Sci. Technol. 41 (2006) 149–165.
[15] A. Rahmani, H.Z. Mousavi, M. Fazli, Effect of nanostructure alumina on adsorption of heavy metals, Desalination 253 (2010) 94–100.
[16] P. Castaldi, M. Silvetti, L. Santona, S. Enzo, P. Melis, XRD, FTIR, and thermal analysis of bauxite ore-processing waste (red mud) exchanged with heavy metals, Clays Clay Miner. 56 (2008) 461–469.
[17] T. Kameda, H. Takeuchi, T. Yoshioka, Uptake of heavy metal ions from aqueous solution using Mg–Al layered double hydroxides intercalated with citrate, malate, and tartrate, Sep. Purif. Technol. 62 (2008) 330–336.
[18] Y.G. Ko, Y.J. Chun, C.H. Kim, U.S. Choi, Removal of Cu(II) and Cr(VI) ions from aqueous solution using chelating fiber packed column: equilibrium and kinetic studies, J. Hazard. Mater. 194 (2011) 92–99.
[19] Y. Zhang, Y.F. Li, L.Q. Yang, X.J. Ma, L.Y. Wang, Z.F. Ye, Characterization and adsorption mechanism of Zn^{2+} removal by PVA/EDTA resin in polluted water, J. Hazard. Mater. 178 (2010) 1046–1054.
[20] C. Liu, R. Bai, Q. San Ly, Selective removal of copper and lead ions by diethylenetriamine-functionalized adsorbent: behaviors and mechanisms, Water Res. 42 (2008) 1511–1522.
[21] X. Wang, Y. Zheng, A. Wang, Fast removal of copper ions from aqueous solution by chitosan-g-poly(acrylic acid)/attapulgite composites, J. Hazard. Mater. 168 (2009) 970–977.
[22] M.V. Dinu, E.S. Dragan, A.W. Trochimczuk, Sorption of Pb(II), Cd(II) and Zn(II) by iminodiacetate chelating resins in non-competitive and competitive conditions, Desalination 249 (2009) 374–379.
[23] P.K. Roy, A.S. Rawat, P.K. Rai, Synthesis, characterisation and evaluation of polydithiocarbamate resin supported on macroreticular styrene–divinylbenzene copolymer for the removal of trace and heavy metal ions, Talanta 59 (2003) 239–246.
[24] A. Ramesh, K. Rama Mohan, K. Seshaiah, Preconcentration of trace metals on Amberlite XAD-4 resin coated with dithiocarbamates and determination by inductively coupled plasma-atomic emission spectrometry in saline matrices, Talanta 57 (2002) 243–252.
[25] L. Niu, S. Deng, G. Yu, J. Huang, Efficient removal of Cu(II), Pb(II), Cr(VI) and As(V) from aqueous solution using an aminated resin prepared by surface-initiated atom transfer radical polymerization, Chem. Eng. J. 165 (2010) 751–757.
[26] L. Yang, Y. Li, X. Jin, Z. Ye, X. Ma, L. Wang, Y. Liu, Synthesis and characterization of a series of chelating resins containing amino/imino–carboxyl groups and their adsorption behavior for lead in aqueous phase, Chem. Eng. J. 168 (2011) 115–124.
[27] C. Ji, S. Song, C. Wang, C. Sun, R. Qu, C. Wang, H. Chen, Preparation and adsorption properties of chelating resins containing 3-aminopyridine and hydrophilic spacer arm for Hg(II), Chem. Eng. J. 165 (2010) 573–580.
[28] L. Li, F. Liu, X. Jing, P. Ling, A. Li, Displacement mechanism of binary competitive adsorption for aqueous divalent metal ions onto a novel IDA-chelating resin: isotherm and kinetic modeling, Water Res. 45 (2011) 1177–1188.
[29] R. Say, E. Birlik, A. Denizli, A. Ersoz, Removal of heavy metal ions by dithiocarbamate-anchored polymer/organosmectite composites, Appl. Clay Sci. 31 (2006) 298–305.
[30] P.K. Roy, A.S. Rawat, P.K. Rai, Synthesis characterisation and evaluation of polydithiocarbamate resin supported on macroreticular styrene–divinylbenzene copolymer for the removal of trace and heavy metal ions, Talanta 59 (2003) 239–246.
[31] L. Dong, Z. Zhu, H. Ma, Y. Qiu, J. Zhao, Simultaneous adsorption of lead and cadmium on MnO_2-loaded resin, J. Environ. Sci. 22 (2010) 225–229.
[32] C.V. Diniz, F.M. Doyle, V.S.T. Ciminelli, Effect of pH on the adsorption of selected heavy metal ions from concentrated chloride solutions by the chelating resin Dowex M-4195, Sep. Sci. Technol. 37 (2002) 3169–3185.
[33] S. Nagib, K. Inoue, T. Yamaguchi, T. Tamaru, Recovery of Ni from a large excess of Al generated from spent hydrodesulfurization catalyst using picolylamine type chelating resin and complexane types of chemically modified chitosan, Hydrometallurgy 51 (1999) 73–85.
[34] S. Song, C. Ji, M. Wang, C. Wang, C. Sun, R. Qu, C. Wang, H. Chen, Adsorption of silver(I) from aqueous solution by chelating resins with 3-aminopyridine and hydrophilic spacer arms: equilibrium, kinetic, thermodynamic, and mechanism studies, J. Chem. Eng. Data 56 (2011) 1001–1008.
[35] L.Q. Yang, Y.F. Li, L.Y. Wang, Y. Zhang, X.J. Ma, Z.F. Ye, Preparation and adsorption performance of a novel bipolar PS-EDTA resin in aqueous phase, J. Hazard. Mater. 180 (2010) 98–105.
[36] Y. Niu, S. Feng, Y. Ding, R. Qu, D. Wang, J. Han, Theoretical investigation on sulfur-containing chelating resin–divalent metal complexes, Int. J. Quantum Chem. 110 (2010) 1982–1993.
[37] L. Song, X. Zhao, J. Fu, X. Wang, Y. Sheng, X. Liu, DFT investigation of Ni(II) adsorption onto MA–DTPA/PVDF chelating membrane in the presence of coexistent cations and organic acids, J. Hazard. Mater. 199–200 (2012) 433–439.
[38] F. Tarazona-Vasquez, P.B. Balbuena, Ab initio study of the lowest energy conformers and IR spectra of poly(amidoamine)-G0 dendrimers, J. Phys. Chem. B 108 (2004) 15982–15991.
[39] P. Comba, S. Knoppe, B. Martin, G. Rajaraman, C. Rolli, B. Shapiro, T. Stork, Copper(II)-mediated aromatic ortho-hydroxylation: a hybrid DFT and ab initio exploration, Chem.-Eur. J. 14 (2008) 344–357.
[40] V.L. Furer, I.I. Vandyukova, J.P. Majoral, A.M. Caminade, V.I. Kovalenko, DFT study of the structure and IR spectra of Gc1 model compound built from cyclotriphosphazene core, J. Mol. Struct. 875 (2008) 587–593.
[41] J.C. Amicangelo, Theoretical characterization of a tridentate photochromic Pt(II) complex using-density functional theory methods, J. Chem. Theory Comput. 3 (2007) 2198–2209.
[42] M. Pavelka, M.K. Shukla, J. Leszczynski, J.V. Burda, Theoretical study of hydrated copper(II) interactions with guanine: a computational density functional theory study, J. Phys. Chem. A 112 (2008) 256–267.
[43] L. Chen, T. Liu, C.a. Ma, Metal complexation and biodegradation of EDTA and S, S-EDDS: a density functional theory study, J. Phys. Chem. A 114 (2010) 443–454.
[44] S.R. Kanel, B. Manning, L. Charlet, H. Choi, Removal of arsenic(III) from groundwater by nanoscale zero-valent iron, Environ. Sci. Technol. 39 (2005) 1291–1298.
[45] H. Genc-Fuhrman, J.C. Tjell, D. McConchie, Adsorption of arsenic from water using activated neutralized red mud, Environ. Sci. Technol. 38 (2004) 2428–2434.
[46] S.L. Sun, L. Wang, A.Q. Wang, Adsorption properties of crosslinked carboxymethyl-chitosan resin with Pb(II) as template ions, J. Hazard. Mater. 136 (2006) 930–937.
[47] M. Gauthier, P.C. Frank, Sub-micron pellicular resins as polymer supports, React. Funct. Polym. 31 (1996) 67–79.
[48] G.S. Kürkçüoğlu, O.Z. Yeşilel, İ. Kavlak, O. Büyükgüngör, Nickel(II) π interaction in [M(ampy)2Ni(μ-CN)2(CN)2]n (M = Zn(II) and Cd(II), ampy = 2-aminomethylpyridine): syntheses, vibrational spectroscopy, thermal analyses and crystal structures of cyano-bridged heteronuclear polymeric complexes, J. Mol. Struct. 920 (2009) 220–226.
[49] X. Zhao, L. Song, Z. Zhang, R. Wang, J. Fu, Adsorption investigation of MA-DTPA chelating resin for Ni(II) and Cu(II) using experimental and DFT methods, J. Mol. Struct. 986 (2011) 68–74.
[50] K.S.W. Sing, D.H. Everett, R.A.W. Haul, L. Moscou, R.A. Pierotti, J. Rouquerol, T. Siemieniewska, Reporting physisorption data for gas solid systems with special reference to the determination of surface-area and porosity (recommendations 1984), Pure. Appl. Chem. 57 (1985) 603–619.
[51] N. Ma, Y. Yang, S. Chen, Q. Zhang, Preparation of amine group-containing chelating fiber for thorough removal of mercury ions, J. Hazard. Mater. 171 (2009) 288–293.
[52] R.J.J. Jansen, H. van Bekkum, XPS of nitrogen-containing functional groups on activated carbon, Carbon 33 (1995) 1021–1027.
[53] T. Tsubota, K. Takenaka, N. Murakami, T. Ohno, Performance of nitrogen- and sulfur-containing carbon material derived from thiourea and formaldehyde as electrochemical capacitor, J. Power Sources 196 (2011) 10455–10460.
[54] K. Dorota, The effects of the treatment conditions on metal ions removal in the presence of complexing agents of a new generation, Desalination 263 (2010) 159–169.
[55] C.Y. Chen, M.S. Lin, K.R. Hsu, Recovery of Cu(II) and Cd(II) by a chelating resin containing aspartate groups, J. Hazard. Mater. 152 (2008) 986–993.
[56] D.K. Kweon, J.K. Choi, E.K. Kim, S.T. Lim, Adsorption of divalent metal ions by succinylated and oxidized corn starches, Carbohydr. Polym. 46 (2001) 171–177.
[57] A. Koseoğlu, E. Kraka, O. Serindağ, T. Varnali, Comparison of Ni, Pd, Pt complexes of N, N-bis(dialkylphosphinomethyl)aminomethane: a DFT study, J. Mol. Struct. Theochem. 896 (2009) 49–53.
[58] J.K. Romary, J.D. Barger, J.E. Bunds, New multidentate alpha-pyridyl ligand. Coordination of bis(2-pyridylmethyl)amine with transition metal ions, Inorg. Chem. 7 (1968) 1142–1145.
[59] W.D. Henry, D.Y. Zhao, A.K. SenGupta, C. Lange, Preparation and characterization of a new class of polymeric ligand exchangers for selective removal of trace contaminants from water, React. Funct. Polym. 60 (2004) 109–120.
[60] E.T.J. Strong, S.A. Cardile, A.L. Brazeau, M.C. Jennings, R. McDonald, N.D. Jones, Chiral, hemilabile palladium(II) complexes of tridentate oxazolidines, including C(2)-symmetric "Pincers", Inorg. Chem. 47 (2008) 10575–10586.
[61] A. Mokhir, R. Stiebing, R. Kraemer, Peptide nucleic acid-metal complex conjugates: facile modulation of PNA–DNA duplex stability, Bioorg. Med. Chem. Lett. 13 (2003) 1399–1401.
[62] A.K. Sengupta, Y.W. Zhu, D. Hauze, Metal(II) ion binding onto chelating exchangers with nitrogen donor atoms: some new observations and related implications, Environ. Sci. Technol. 25 (1991) 481–488.